

Quantifying the Impact of Microphonics in High-Q Experiments for Dark Sector Searches

Stephen E. Henrich
Graduate Student
UMN Department of Physics

Collaborators: Zhen Liu and Saarik Kalia
10/14/2023

What is Dark SRF?



UNIVERSITY OF MINNESOTA

A dark photon search experiment using state-of-the-art superconducting radiofrequency (SRF) cavities, with quality factors (Q) of 10^{10}

Oscillating EM fields are a source of dark photons and vice versa

$$\mathcal{L} \supset -\frac{1}{4} F'^{\mu\nu} F'_{\mu\nu} + \frac{1}{2} m_{A'}^2 A'^{\mu} A'_{\mu} + \overbrace{\epsilon e A'^{\mu} J_{\mu}^{EM}}^{\text{Interaction w/ ordinary EM fields}}$$

Dark photon *Kinetic mixing parameter*

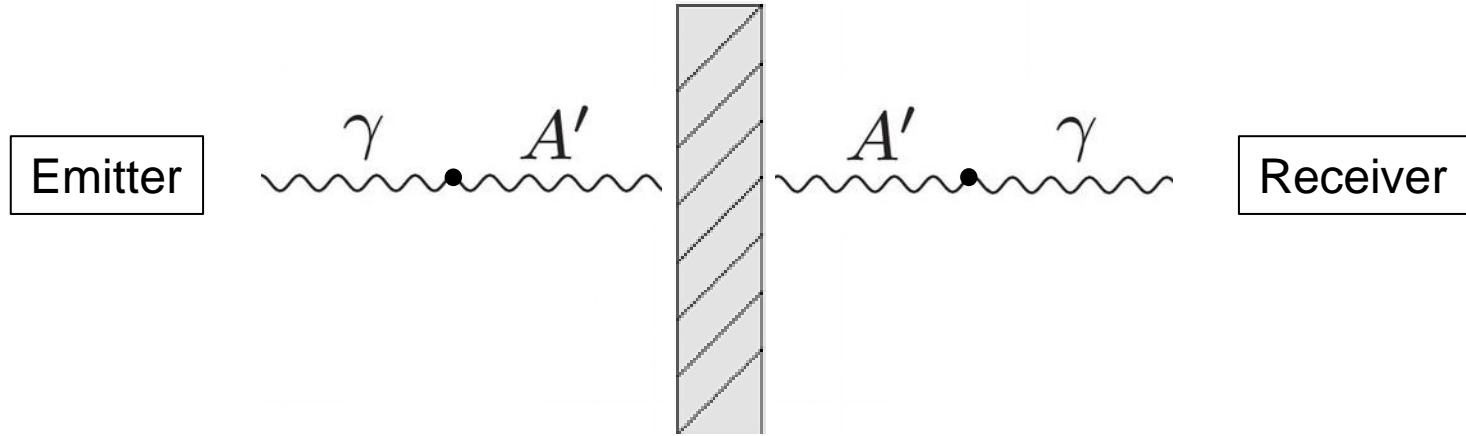
Experimental setup: Light-shining-through-wall (LSW) experiment



 Fermilab



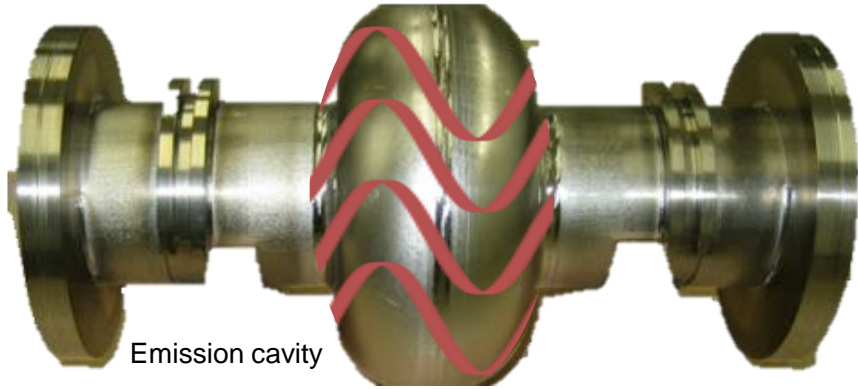
Light shining through walls (LSW)



“Walls” are impenetrable to ordinary light, but penetrable to dark photons
After passing through the wall, some dark photons convert back to ordinary photons observed by a detector



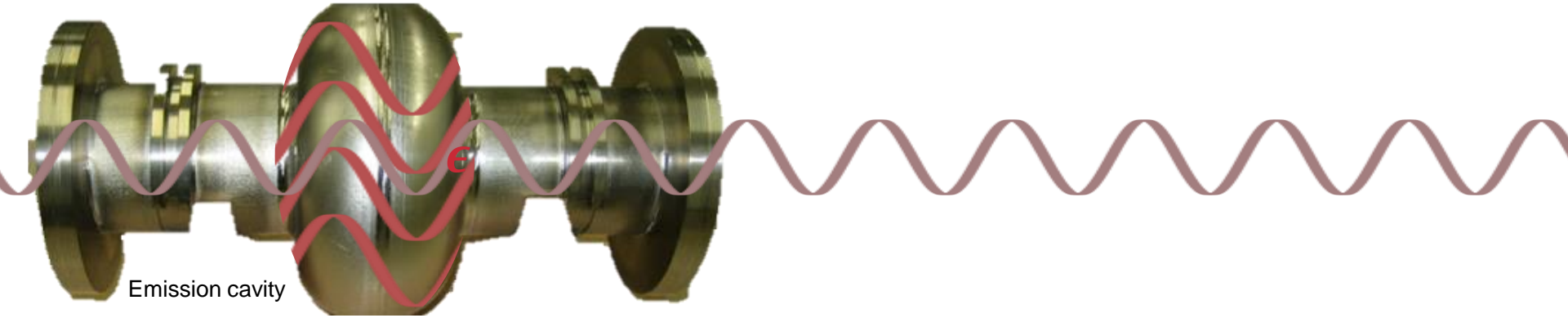
SRF for Dark Photon



Power it up:

- 40 MV/m (26 J stored energy)
- $\sim 10^{25}$ photons

SRF for Dark Photon



Power it up:

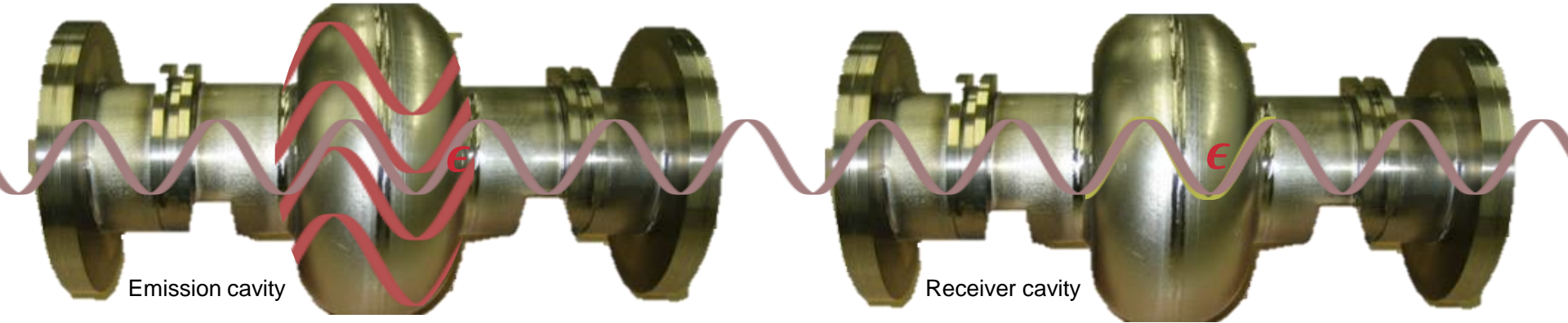
- 40 MV/m (26 J stored energy)
- $\sim 10^{25}$ photons

SM photon does not penetrate the superconducting wall.
But dark photons can!

Dark photon field:

$$\vec{E}'(\vec{r}, t) \simeq -\epsilon m_{\gamma'}^2 \int_{V_{\text{emitter}}} d^3x \frac{\vec{E}_{\text{cav}}(\vec{x})}{4\pi|\vec{r}-\vec{x}|} e^{i(\omega t - k|\vec{r}-\vec{x}|)}$$

SRF for Dark Photon



Power it up:

- 40 MV/m (26 J stored energy)
- $\sim 10^{25}$ photons

SM photon does not penetrate the superconducting wall.
But dark photons can!

Dark photon field:

$$\vec{E}'(\vec{r}, t) \simeq -\epsilon m_{\gamma'}^2 \int_{V_{\text{emitter}}} d^3x \frac{\vec{E}_{\text{cav}}(\vec{x})}{4\pi|\vec{r}-\vec{x}|} e^{i(\omega t - k|\vec{r}-\vec{x}|)}$$

Induced effective current

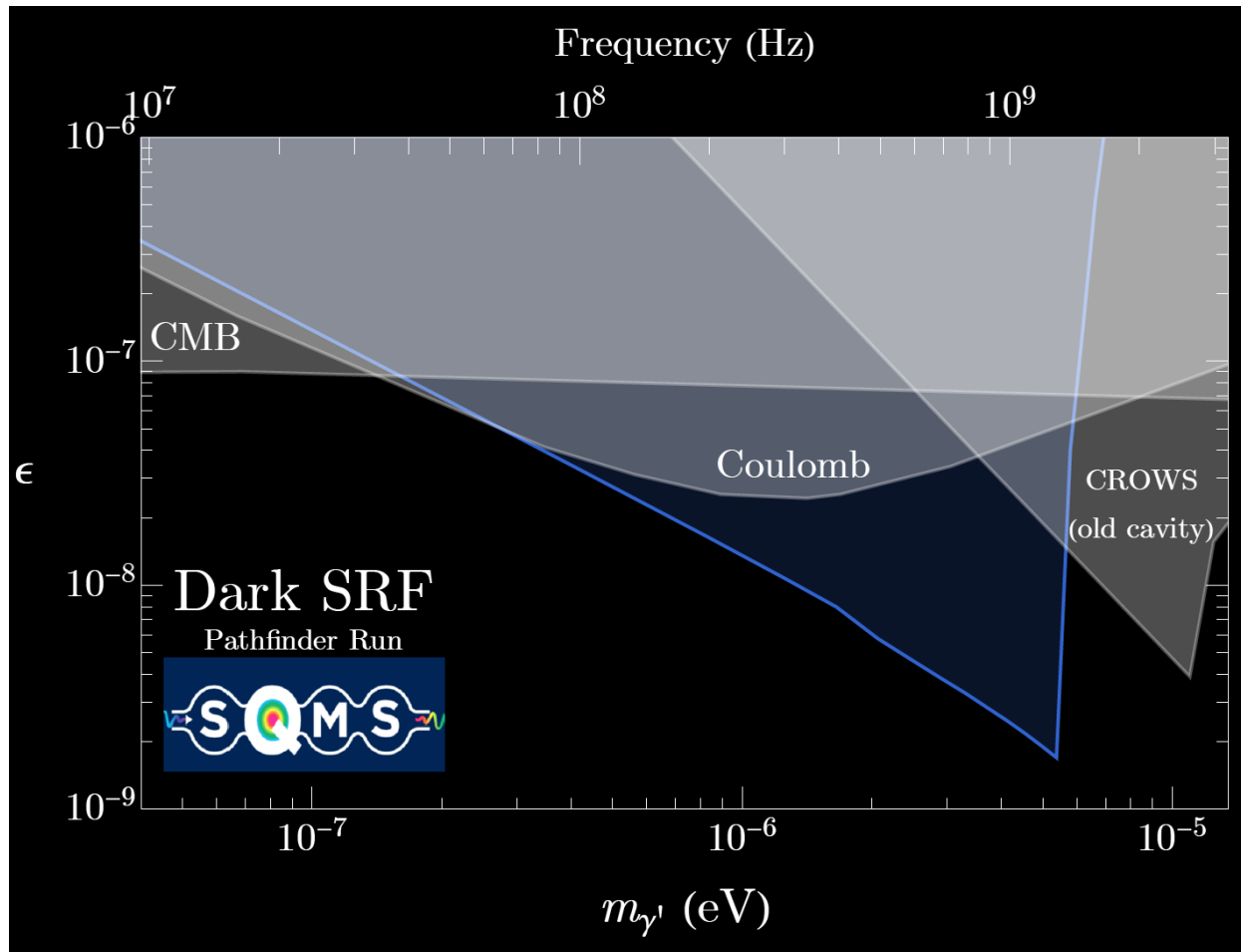
$$\vec{j}(\vec{r})e^{i\omega t} = -\frac{i\epsilon}{\omega} \left(m_{\gamma'}^2 \vec{E}' - \vec{\nabla}(\vec{\nabla} \cdot \vec{E}') \right)$$

Receiver field:

$$\vec{E}_{\text{receiver}}(\vec{r}, t) = -\frac{Q_{\text{rec}}}{\omega} \left[\frac{\int d^3x \vec{E}_{\text{cav}}^*(\vec{x}) \cdot \vec{j}(\vec{x})}{\int d^3x |\vec{E}_{\text{cav}}(\vec{x})|^2} \right] \vec{E}_{\text{cav}}(\vec{r})e^{i\omega t}$$

Dark SRF: Pathfinder results

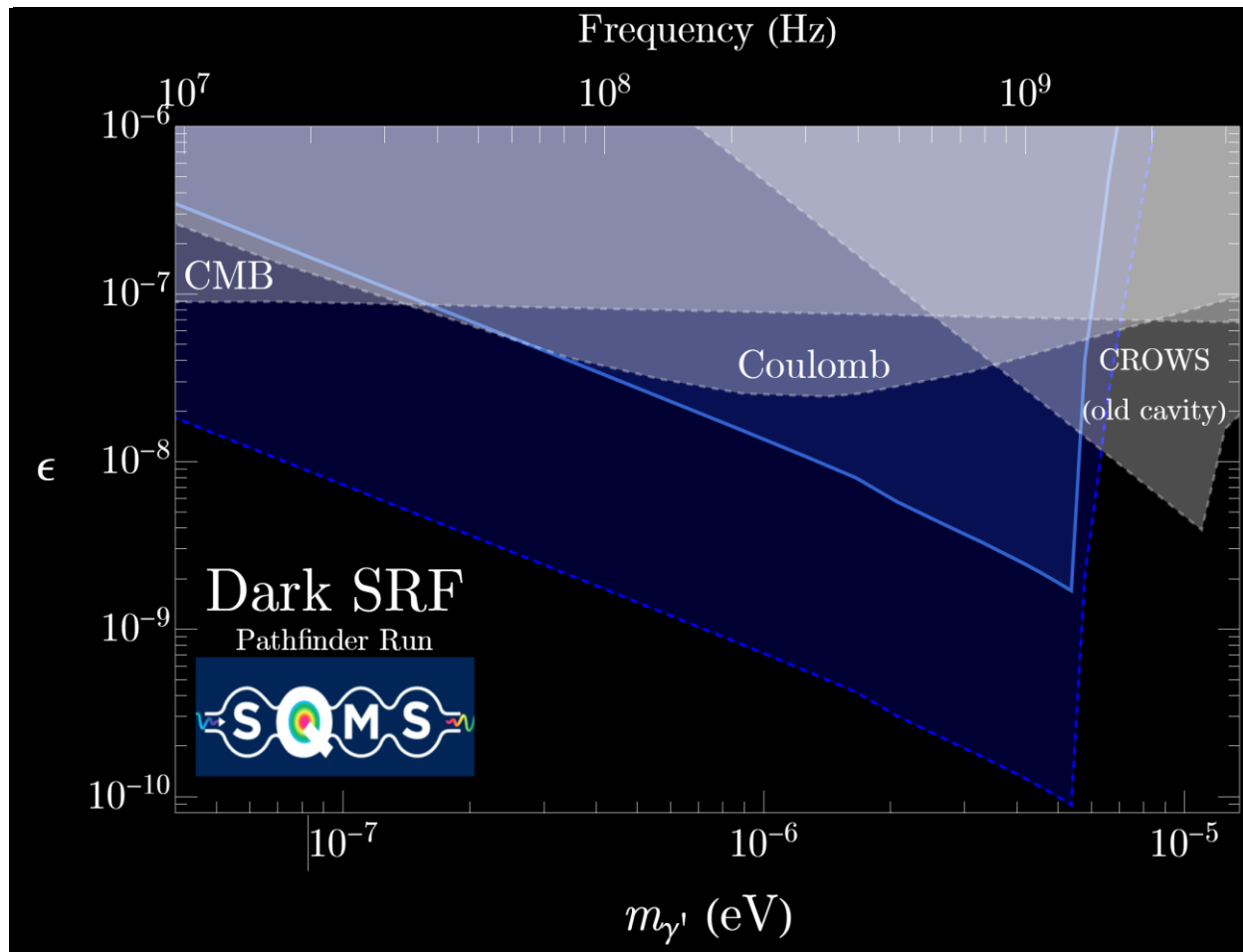
Our pathfinder run results
already explore new territory!



Dark SRF: Pathfinder results

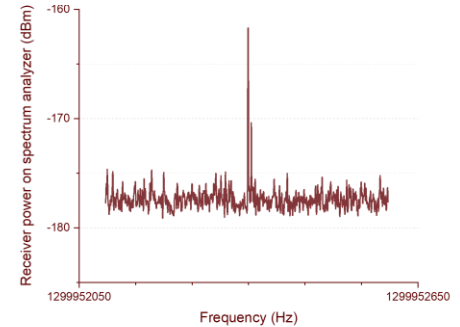
Our pathfinder run results
already explore new territory...

But it could be even better!



High-Q cavities: Finicky friends

Resonator	Quality factor (Q)
Resonant (LC) circuit	$\sim 10^2\text{-}10^6$
Microwave/RF cavity (copper)	$\sim 10^6$
Superconducting radiofrequency (SRF) cavity (e.g. niobium)	$\sim 10^{10}$



SRF Applications: accelerators, cavities, quantum computing architectures, free electron lasers

Advantages

- High energy storage with minimal power loss to cavity walls
- Narrow bandwidth for precision experiments

Disadvantages

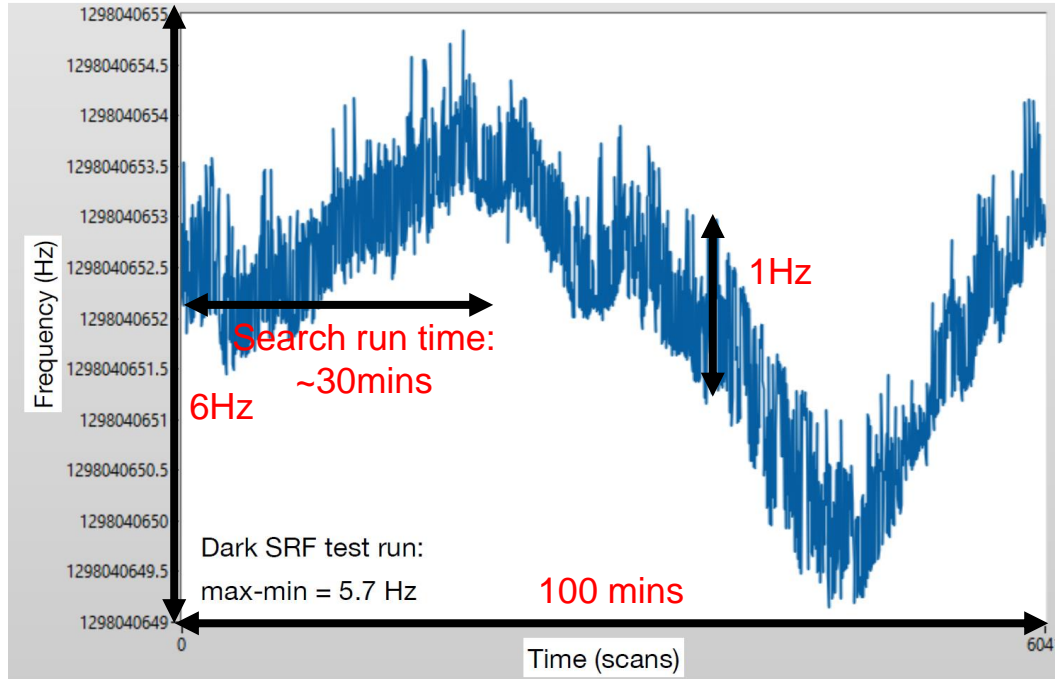
- Vulnerable to frequency drift
- Vulnerable to microphonics

$$Q \propto \frac{\omega}{\gamma} \approx \frac{\text{energy stored}}{\text{energy dissipated per cycle}}$$



SRF technology

Microphonics and frequency drift



$$|G|^2 \rightarrow \frac{\omega^2}{\omega^2 + 4\delta\omega^2 Q_{\text{rec}}^2} |G|^2$$

Initial conservative estimate of frequency drift and microphonics:

- $\delta\omega = 7.8$ Hz, fixed offset from ω_0
- Power suppression: 7.7×10^{-6}

↑
> 100,000-fold loss of signal!



Is the true penalty from microphonics this severe?

Let's try to model microphonics more accurately and find out



A Deceptively Simple Model: Driven, Damped Oscillator

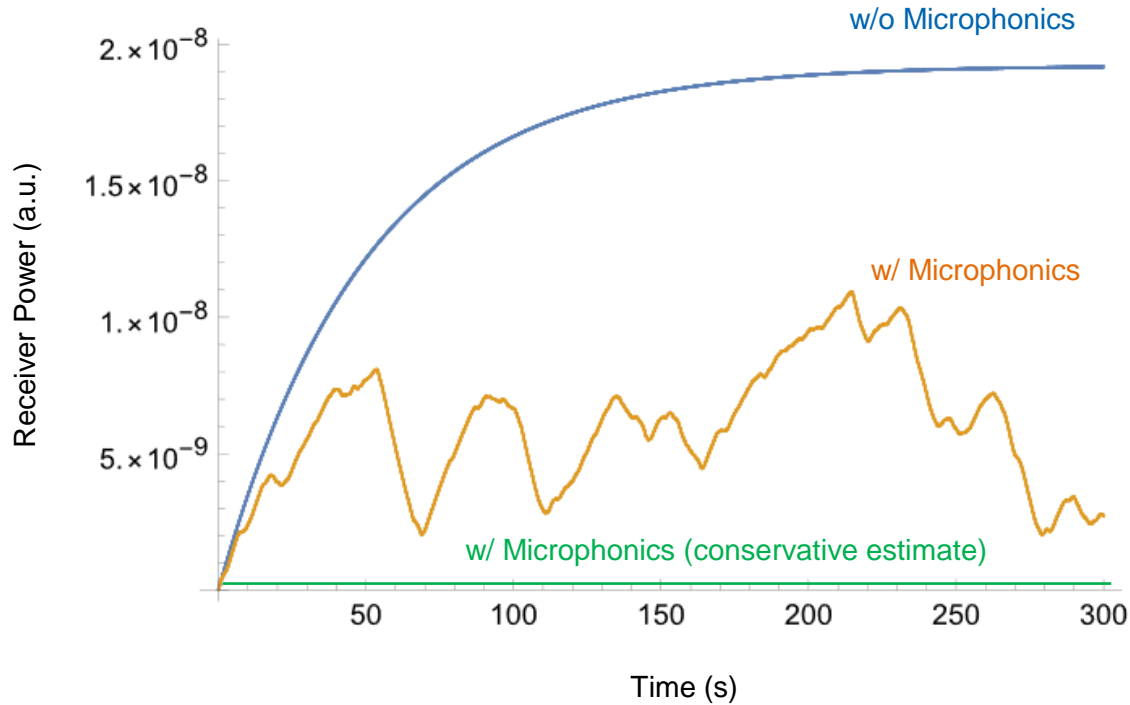
$$\ddot{x}(t) + 2\gamma\dot{x}(t) + (\omega_0 + \delta\omega(t))^2x(t) = \frac{F_0}{m}e^{i\omega_F t}$$

- ω_0 : natural frequency of the receiver cavity (without microphonics)
- γ : damping factor
- ω_F : driving frequency (emission cavity frequency sourcing dark photons)
- $\delta\omega(t)$: microphonics perturbations to the receiver frequency
- τ : jittering time

Parameter Scale:	γ	\ll	$\delta\omega(t)$	\ll	$\frac{1}{\tau}$	\ll	ω_0
------------------	----------	-------	-------------------	-------	------------------	-------	------------

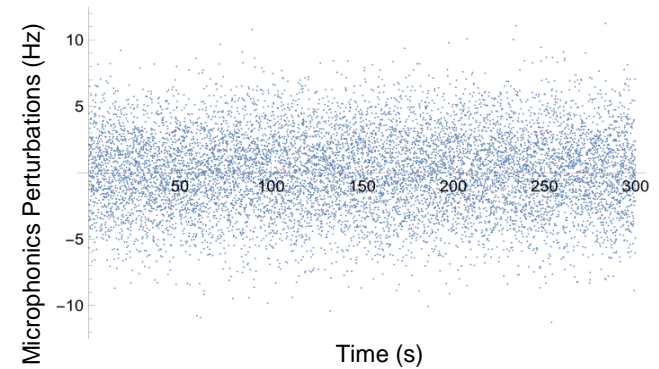


Initial Results: 10,000-fold better than estimated!

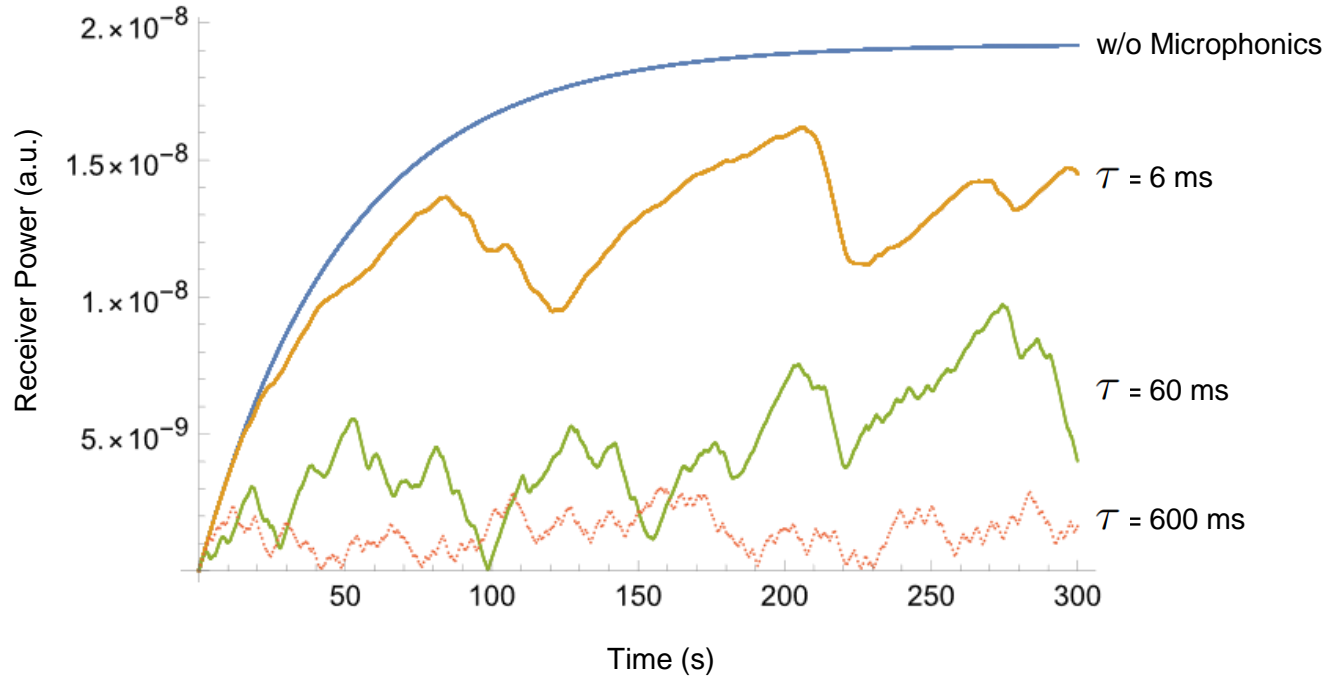


Previous estimate of power retention: $< 0.0001\%$

Power retention using microphonics modeling: 14.67%

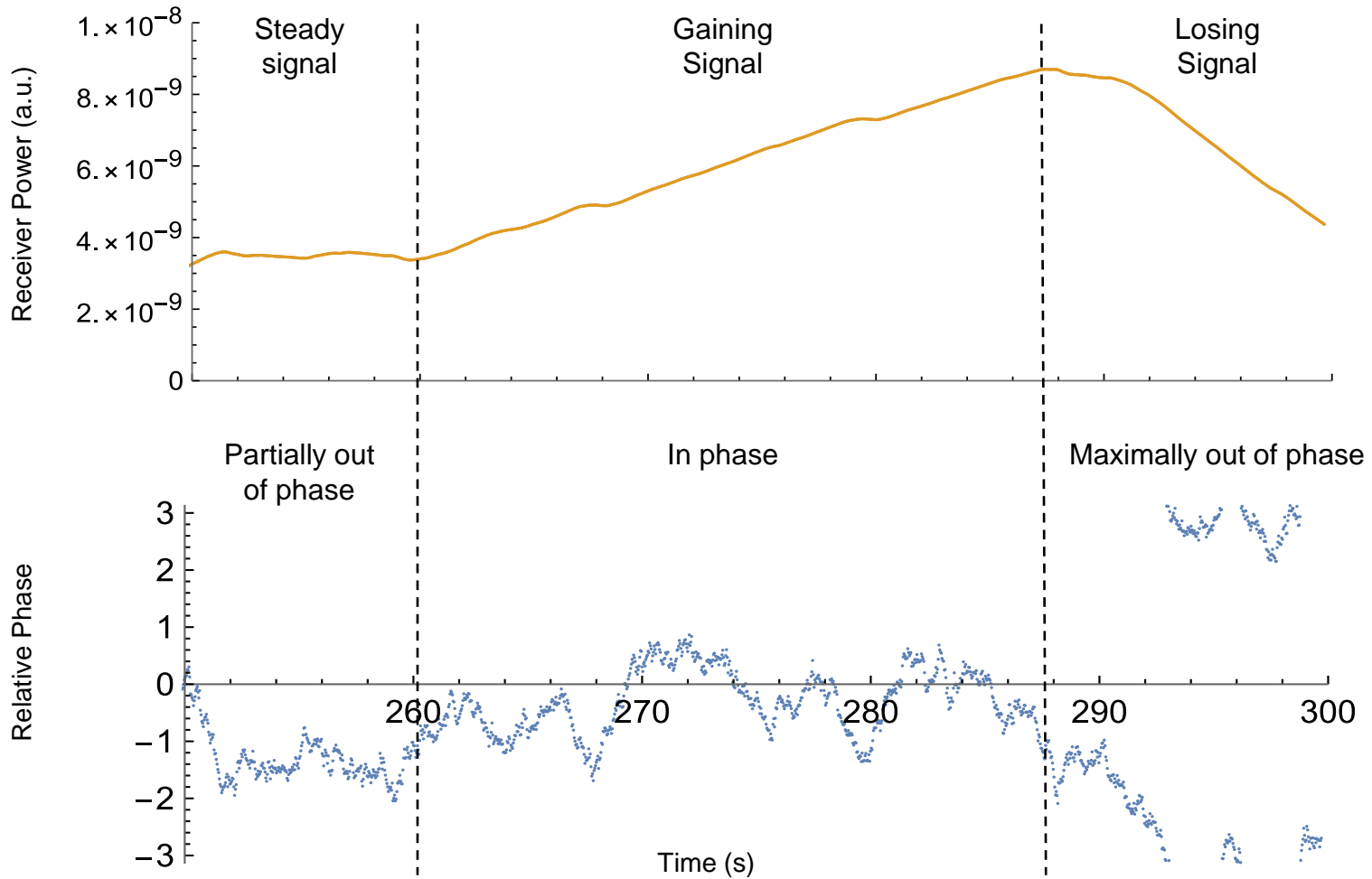


Rate of jittering has a huge impact



Jittering time (milliseconds)	Normalized Receiver Power
None	1
6	0.54
60	0.092
600	0.0087





Summary and Conclusions

- SRF cavities offer great precision and sensitivity for dark sector searches, but are vulnerable to frequency instability due to microphonics
- The precise impact of microphonics in dark SRF experiments had not previously been quantified
- Correct microphonics modeling could improve SNR by 10^5
- Microphonics effects may be dictated by the accumulated relative phase between the receiver and the dark photon source



Thank you!



Dark photon Lagrangian

$$\mathcal{L} = -\frac{1}{4}(f_{\mu\nu}f^{\mu\nu} + f'_{\mu\nu}f'^{\mu\nu} - 2\varepsilon f_{\mu\nu}f'^{\mu\nu}) + \frac{1}{2}m_{\gamma'}^2 a'_\mu a'^\mu - e a_\mu j_{EM}^\mu,$$

$$\mathcal{L} = -\frac{1}{4}(F_{\mu\nu}F^{\mu\nu} + F'_{\mu\nu}F'^{\mu\nu}) + \frac{1}{2}m_{\gamma'}^2 A'_\mu A'^\mu - e J_{EM}^\mu (A_\mu + \varepsilon A'_\mu),$$

where A_μ and A'_μ are of course linear combinations of a_μ and a'_μ . The propagating mass eigenstates are the transverse photon and hidden-photon modes $|A_T\rangle$ and $|A'_T\rangle$, along with the longitudinal hidden-photon mode $|A'_L\rangle$ (there is no longitudinal mode for the massless photon). In this basis, the linear combination $|A_T\rangle + \varepsilon|A'_T\rangle$ directly interacts with charges, while the linear combination $|A'_T\rangle - \varepsilon|A_T\rangle$ is sterile.



Equations of Motion (Maxwell and Proca)

The equations of motion for the photon and hidden-photon fields, in the mass basis, follow from Eq. (2), and are given by

$$(\partial_t^2 - \nabla^2)V = \rho_{EM} \quad (\partial_t^2 - \nabla^2)\vec{A} = \vec{j}_{EM} \quad \dot{\vec{V}} + \nabla \cdot \vec{A} = 0, \quad (3)$$

$$(\partial_t^2 - \nabla^2 + m_{\gamma'}^2)V' = \varepsilon \rho_{EM} \quad (\partial_t^2 - \nabla^2 + m_{\gamma'}^2)\vec{A}' = \varepsilon \vec{j}_{EM} \\ \dot{\vec{V}}' + \nabla \cdot \vec{A}' = 0. \quad (4)$$

of Lorenz gauge). Equations (4) are the Proca equations for a massive vector. They show that the massive hidden-photon field is sourced by electric charge density ρ_{EM} and current \vec{j}_{EM} in the same way as the massless photon field, but suppressed by a factor of ε . The final part of Eqs. (4) is a constraint equivalent to conservation of electric charge.

Any setup that produces ordinary electric and magnetic fields will, through Eqs. (4), also source hidden-photon fields at $\mathcal{O}(\varepsilon)$. In turn, the Lorentz force on charged particles receives an ε -suppressed contribution from these hidden-photon fields,

$$\vec{F} = q[(\vec{E} + \varepsilon\vec{E}') + \vec{v} \times (\vec{B} + \varepsilon\vec{B}')] \\ \text{(modified Lorentz force).}$$



E and B Fields

A. General prescription for an arbitrary experimental geometry

Take $\vec{E}(\vec{r}, t) = \vec{E}_{em}(\vec{r})e^{i\omega t}$ and $\vec{B}(\vec{r}, t) = \vec{B}_{em}(\vec{r})e^{i\omega t}$ to be the (known) E - and B -fields of the cavity mode that is driven inside the emitter cavity. The emitter cavity then radiates a hidden-photon field, with the hidden electric field \vec{E}' given by

$$\vec{E}'(\vec{r}, t) = -\epsilon m_\gamma^2 \left[\int_{em} d^3x \frac{\vec{E}_{em}(\vec{x})}{4\pi|\vec{r}-\vec{x}|} e^{-ik|\vec{r}-\vec{x}|} \right] e^{i\omega t}. \quad (24)$$

Here the integral is over the interior of the emitter-cavity,

The hidden-photon fields penetrate the receiver cavity, where they excite a resonant response of the matching receiver-cavity mode. After allowing $\sim 2\pi Q$ cycles for the resonance to ring up, the observed signal fields within the receiver cavity are given by⁶

$$\vec{E}_{\text{observed}}(\vec{r}, t) = -\frac{Q}{\omega} \left[\frac{\int_{\text{rec}} d^3x \vec{E}_{\text{cav}}^*(\vec{x}) \cdot \vec{J}_{\text{eff}}(\vec{x})}{\int_{\text{rec}} d^3x |E_{\text{cav}}(\vec{x})|^2} \right] \vec{E}_{\text{cav}}(\vec{r}) e^{i\omega t} \quad (25)$$

$$\vec{B}_{\text{observed}}(\vec{r}, t) = -\frac{Q}{\omega} \left[\frac{\int_{\text{rec}} d^3x \vec{E}_{\text{cav}}^*(\vec{x}) \cdot \vec{J}_{\text{eff}}(\vec{x})}{\int_{\text{rec}} d^3x |E_{\text{cav}}(\vec{x})|^2} \right] \vec{B}_{\text{cav}}(\vec{r}) e^{i\omega t} \quad (26)$$

$$\vec{J}_{\text{eff}}(\vec{x}) \equiv -\frac{i\epsilon}{\omega} [m_\gamma^2 \vec{E}'(\vec{x}, 0) - \vec{\nabla}(\vec{\nabla} \cdot \vec{E}'(\vec{x}, 0))]. \quad (27)$$



E & B Fields: Transverse vs Longitudinal Modes

The hidden-photon fields penetrate the receiver cavity, where they excite a resonant response of the matching receiver-cavity mode. After allowing $\sim 2\pi Q$ cycles for the resonance to ring up, the observed signal fields within the receiver cavity are given by⁶

$$\vec{E}_{\text{observed}}(\vec{r}, t) = -\frac{Q}{\omega} \left[\frac{\int_{\text{rec}} d^3x \vec{E}_{\text{cav}}^*(\vec{x}) \cdot \vec{J}_{\text{eff}}(\vec{x})}{\int_{\text{rec}} d^3x |E_{\text{cav}}(\vec{x})|^2} \right] \vec{E}_{\text{cav}}(\vec{r}) e^{i\omega t} \quad (25)$$

$$\vec{B}_{\text{observed}}(\vec{r}, t) = -\frac{Q}{\omega} \left[\frac{\int_{\text{rec}} d^3x \vec{E}_{\text{cav}}^*(\vec{x}) \cdot \vec{J}_{\text{eff}}(\vec{x})}{\int_{\text{rec}} d^3x |E_{\text{cav}}(\vec{x})|^2} \right] \vec{B}_{\text{cav}}(\vec{r}) e^{i\omega t} \quad (26)$$

$$\vec{J}_{\text{eff}}(\vec{x}) \equiv -\frac{i\varepsilon}{\omega} [m_\gamma^2 \vec{E}'(\vec{x}, 0) - \vec{\nabla}(\vec{\nabla} \cdot \vec{E}'(\vec{x}, 0))]. \quad (27)$$

The function $\vec{J}_{\text{eff}}(\vec{x})$ appearing above deserves further attention, since it captures the key result of this paper. If the radiated hidden-photon field is purely transverse, then by definition $\vec{\nabla} \cdot \vec{E}' = 0$, whereas if it is purely longitudinal then $\vec{\nabla}(\vec{\nabla} \cdot \vec{E}') = -k^2 \vec{E}'$. In both cases \vec{J}_{eff} simplifies, and we can write

$$\vec{J}_{\text{eff}}(\vec{x}) = -\frac{i\varepsilon}{\omega} \vec{E}'(\vec{x}, 0) \times \begin{cases} m_\gamma^2 & \text{(Pure transverse)} \\ \omega^2 & \text{(Pure longitudinal)} \end{cases} \quad (28)$$

Comparing the two cases, we immediately see the parametric enhancement of the signal from the longitudinal mode over the transverse mode in the small mass limit.



Longitudinal Mode: Epsilon, mass dependence

The mode will thus go through the wall, and since it is directly coupled to electromagnetic currents, it can be detected on the other side. In this setup, the dependence on $m_{\gamma'}$ appears because both the production amplitude of longitudinal modes, and the strength of their effect on electric charges, scales as $m_{\gamma'}/\omega$. Hence, if the longitudinal mode is utilized, the signal in the experiment would scale as $\epsilon^2 m_{\gamma'}^2/\omega^2$, more favorably than the transverse mode. This makes such experiments capable of covering significant new parameter space beyond current bounds (see Fig. 2).

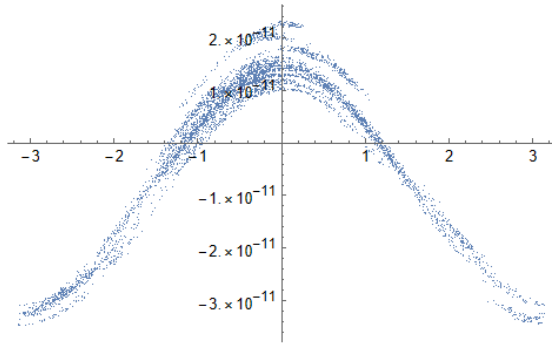


$$\text{SNR} \simeq \frac{P_{\text{signal}} t_{\text{int}}}{T} \simeq \frac{\omega B_{\text{rec}}^2 V_{\text{cav}} t_{\text{int}}}{Q T}.$$

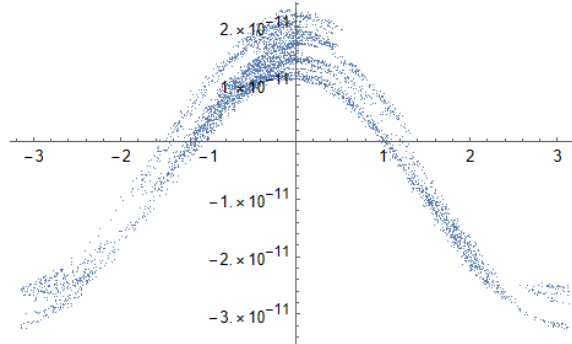


Phase vs Power Gradient

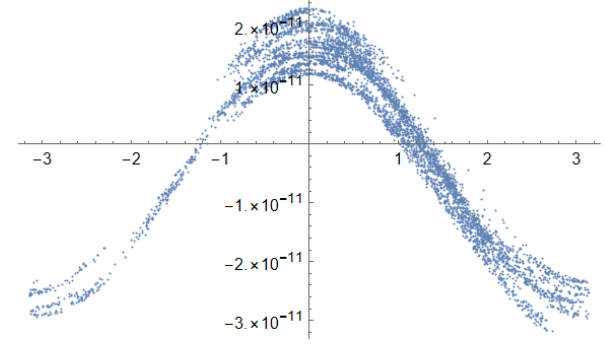
Trial 1



Trial 2



Trial 3

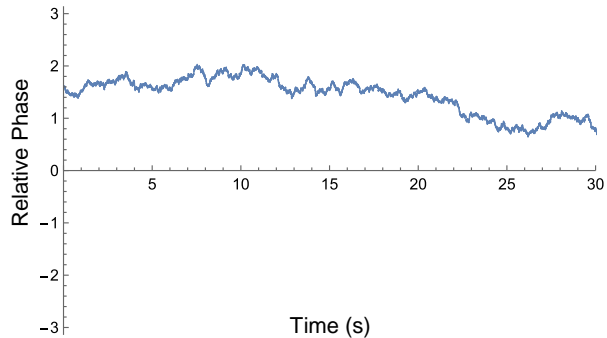


```
In[24]= ListPlot[{{Table[{Arg[(xBCList[[i + 1]] + I * vBCList[[i + 1]] / omega0) * Exp[I * (omega0) * (i * tjit) - I * Pi / 2]], (Abs[xBCList[[i + 2]]] - Abs[xBCList[[i]])}], {i, 0, num - 2}}]}
```

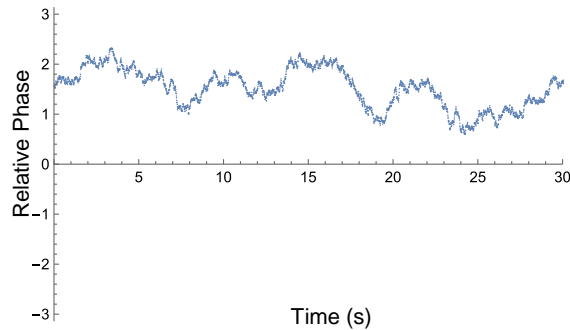


Relative Phase Change (tjit dependence)

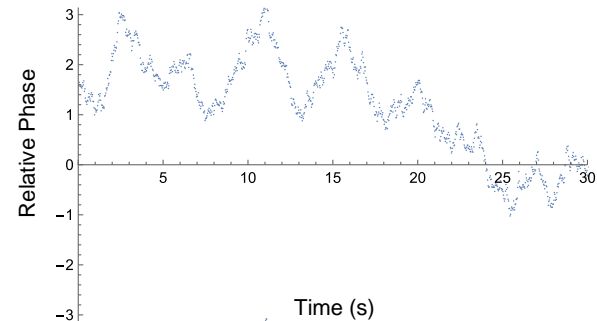
Tjit=0.00333; t = 30s



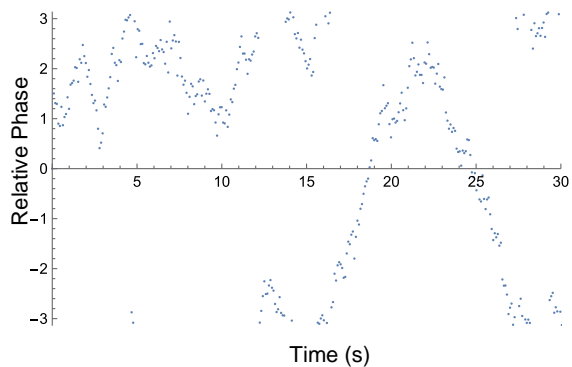
Tjit=0.01; t = 30s



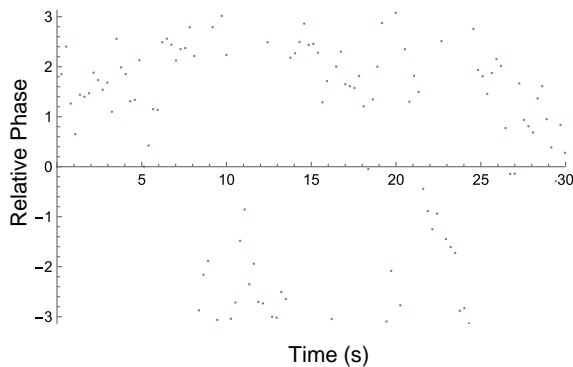
Tjit=0.03; t = 30s



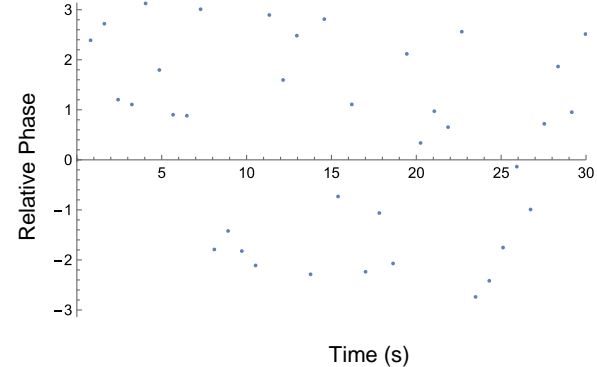
Tjit=0.09; t = 30s



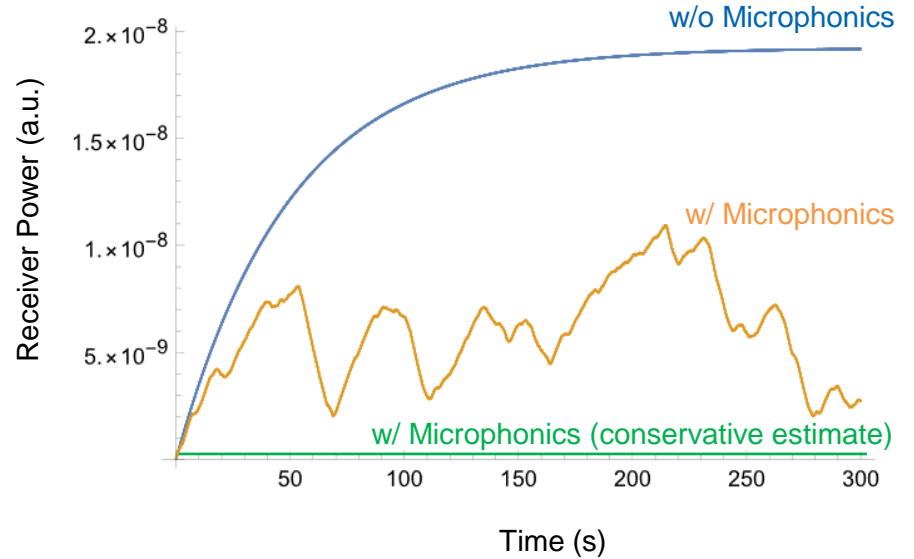
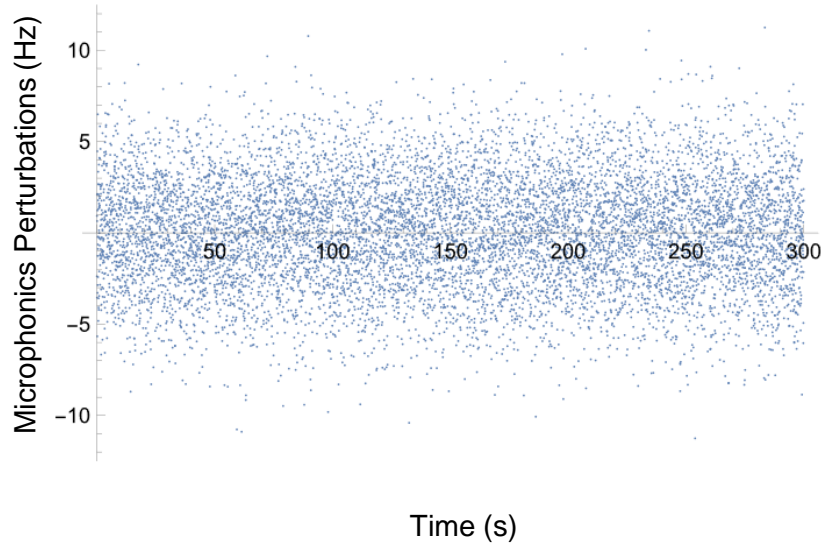
Tjit=0.27; t = 30s



Tjit=0.81; t = 30s



Initial Results: 10,000-fold better than estimated!



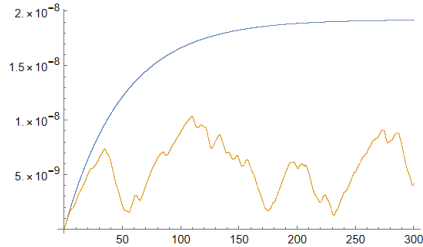
Estimated Power Retention: 0.0001%

Power Retention: 14.67%



Rate of jittering has a huge impact

Tjitter = 0.03



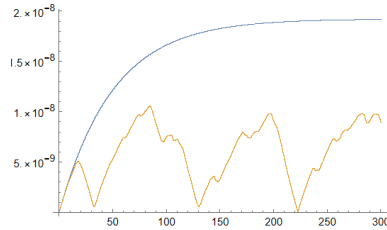
$\{3.00045 \times 10^8, 2.77691 \times 10^{-12}\}$

$\{3.00045 \times 10^8, 3.65571 \times 10^{-13}\}$

$\{1., 0.131647\}$

Power
Suppression

Tjitter = 0.015

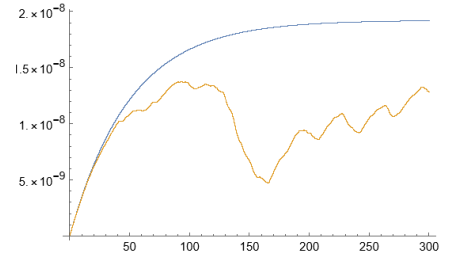


$\{6.00045 \times 10^8, 5.55363 \times 10^{-12}\}$

$\{6.00045 \times 10^8, 8.60076 \times 10^{-13}\}$

$\{1., 0.154867\}$

Tjitter = 0.0075

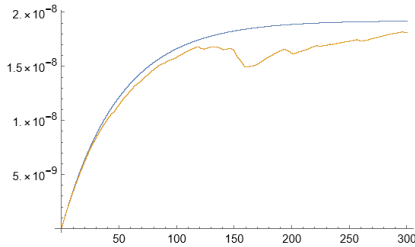


$\{1.20005 \times 10^9, 1.11071 \times 10^{-11}\}$

$\{1.20005 \times 10^9, 4.22738 \times 10^{-12}\}$

$\{1., 0.380602\}$

Tjitter = 0.003



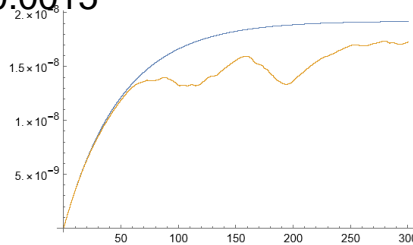
$\{3.00005 \times 10^9, 2.77674 \times 10^{-11}\}$

$\{3.00005 \times 10^9, 2.29419 \times 10^{-11}\}$

$\{1., 0.826217\}$

Power
Suppression

Tjitter = 0.0015

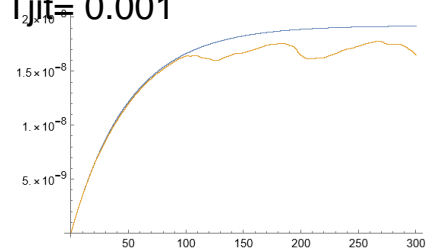


$\{6.00005 \times 10^9, 5.55346 \times 10^{-11}\}$

$\{6.00005 \times 10^9, 3.96694 \times 10^{-11}\}$

$\{1., 0.714318\}$

Tjitter = 0.001



$\{9.00005 \times 10^9, 8.33019 \times 10^{-11}\}$

$\{9.00005 \times 10^9, 7.08939 \times 10^{-11}\}$

$\{1., 0.851049\}$



The Model: Driven, Damped Oscillator

$$\delta\omega(t) = \begin{cases} -\alpha, & 0 < t < \tau_1 \\ 0, & \tau_1 < t < \tau_2 \\ \alpha, & \tau_2 < t < \tau_3 \end{cases}$$

A simple starting point: consider discrete time intervals (on the order of 20-30 milliseconds) with constant frequency mismatch

Plan: Obtain a solution for a single time interval explicitly in terms of boundary conditions, and then stitch the solutions together

Intermediate steps

- Solve the homogeneous equation for a single time interval
- Obtain a particular solution for the sourced (inhomogeneous) equation
- Write the general solution as a sum of the particular solution and a linear combination of the homogeneous solution set



Analytic Solution for a Single Interval

Homogeneous Equation:

$$\ddot{x} + 2\gamma\dot{x} + (\omega_0 + \delta\omega)^2x = 0$$

We use the complex ansatz $x_{tr}(t) = Ce^{-i\omega t}$

Solution:

$$x_{tr}(t) = \psi_+ e^{-i\omega_+ t} + \psi_- e^{-i\omega_- t}$$

$$\omega_{\pm} = -i\gamma \pm \sqrt{(\omega_0 + \delta\omega)^2 - \gamma^2}$$

Inhomogeneous Equation:

$$\ddot{x}(t) + 2\gamma\dot{x}(t) + (\omega_0 + \delta\omega)^2x(t) = \frac{F_0}{m}e^{i\omega_F t}$$

We consider an ansatz of the form: $x_{ss}(t) = Ae^{i(\omega_0 t + \phi)}$

Solution:

$$x_{ss}(t) = Ae^{i(\omega_0 t + \phi)}$$

$$= \frac{F_0}{m} \frac{1}{\sqrt{((\omega_0 + \delta\omega)^2 - \omega_0^2)^2 + 4\gamma^2\omega_0^2}} e^{i(\omega_0 t - \theta)}$$

$$\theta = \tan^{-1} \left(\frac{2\gamma\omega_0}{(\omega_0 + \delta\omega)^2 - \omega_0^2} \right)$$

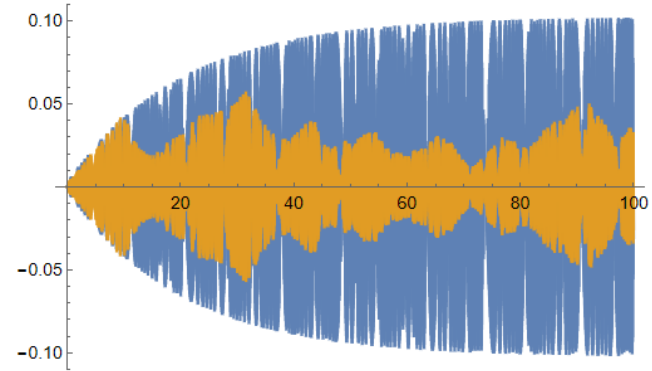


Analytic vs. Numerical Comparison

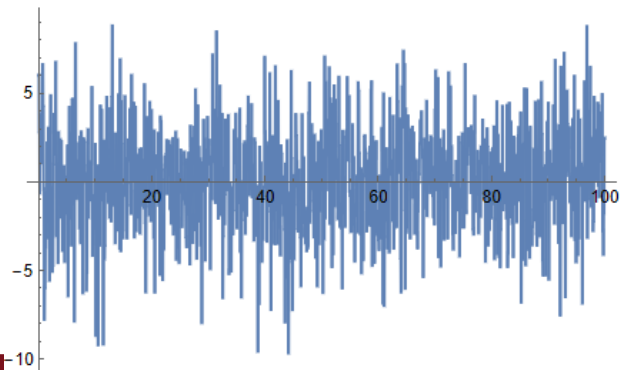
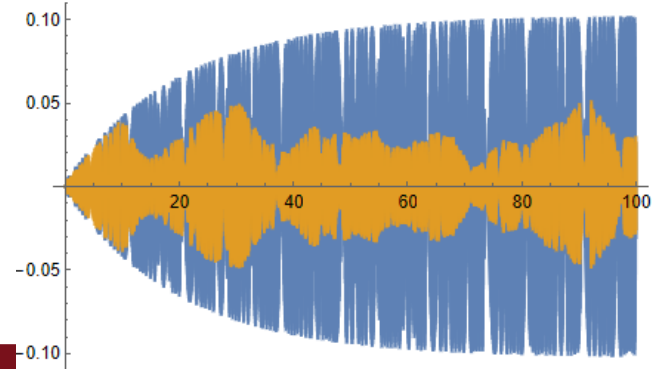
Parameters:

- $\omega_0 = \omega_F = 100$
- $\gamma = 0.1$
- $\tau_{jit} = 0.1$
- $\delta\Omega = 3$
- Microphonics:
RandomVariate[NormDist[0,3],nu
m]
- Time: 100 s (1.66 min)
- # of intervals: 1000

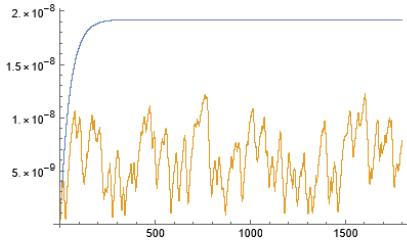
Analytic



Numerical



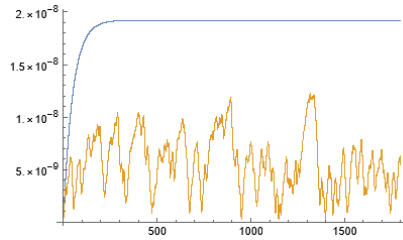
Analytic Physical Model: 30 min runs



{ 6.48016×10^{10} , 2.1265×10^{-11} }

{ 6.48016×10^{10} , 2.72017×10^{-12} }

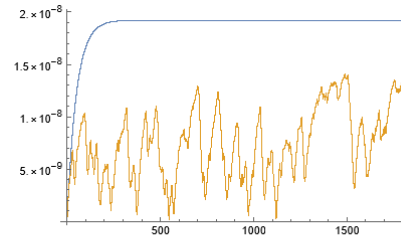
{1., 0.127918}



{ 6.48016×10^{10} , 2.1265×10^{-11} }

{ 6.48016×10^{10} , 2.30133×10^{-12} }

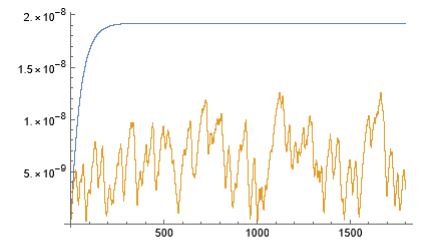
{1., 0.108222}



{ 6.48016×10^{10} , 2.1265×10^{-11} }

{ 6.48016×10^{10} , 3.88498×10^{-12} }

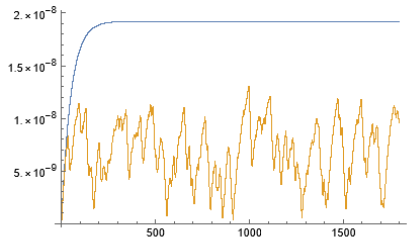
{1., 0.182694}



{ 6.48016×10^{10} , 2.1265×10^{-11} }

{ 6.48016×10^{10} , 2.66214×10^{-12} }

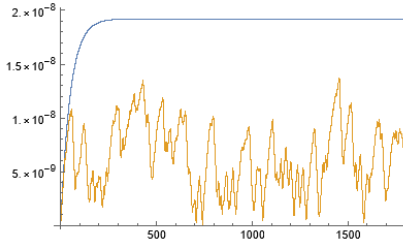
{1., 0.125189}



{ 6.48016×10^{10} , 2.1265×10^{-11} }

{ 6.48016×10^{10} , 3.28581×10^{-12} }

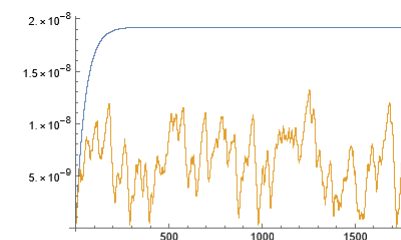
{1., 0.154518}



{ 6.48016×10^{10} , 2.1265×10^{-11} }

{ 6.48016×10^{10} , 2.96986×10^{-12} }

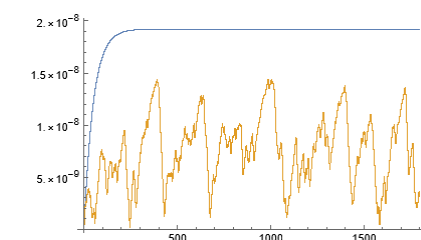
{1., 0.13966}



{ 6.48016×10^{10} , 2.1265×10^{-11} }

{ 6.48016×10^{10} , 2.94711×10^{-12} }

{1., 0.13859}



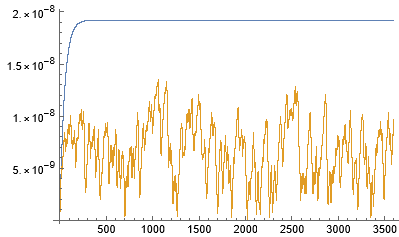
{ 6.48016×10^{10} , 2.1265×10^{-11} }

{ 6.48016×10^{10} , 4.00658×10^{-12} }

{1., 0.188412}



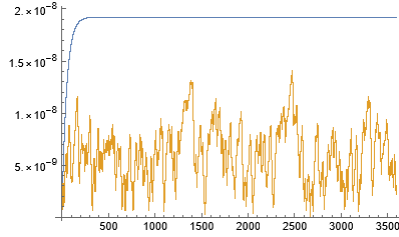
Analytic Physical Model (1 hr runs)



{ 5.18406×10^{11} , 4.34543×10^{-11} }

{ 5.18406×10^{11} , 6.18129×10^{-12} }

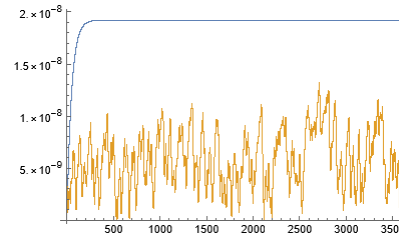
{1., 0.142248}



{ 5.18406×10^{11} , 4.34543×10^{-11} }

{ 5.18406×10^{11} , 5.23355×10^{-12} }

{1., 0.120438}



{ 5.18406×10^{11} , 4.34543×10^{-11} }

{ 5.18406×10^{11} , 4.90664×10^{-12} }

{1., 0.112915}

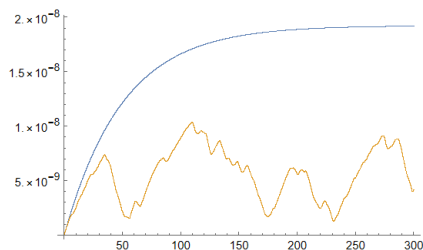
Average Power Suppression Factor: 0.13-0.14

Why? What is driving the power suppression? Why is the suppression tjit-dependent?



Tjit-Dependence (5 min runs); Rand[NormDist[0,3]]

Tjit= 0.03

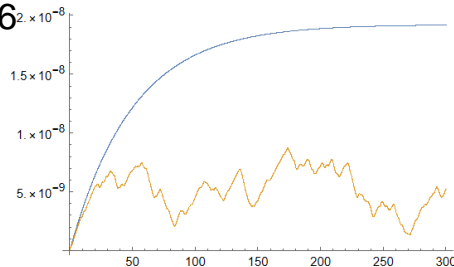


{3.00045 × 10⁸, 2.77691 × 10⁻¹²}
 {3.00045 × 10⁸, 3.65571 × 10⁻¹³}

{1., 0.131647}

Power
Suppression

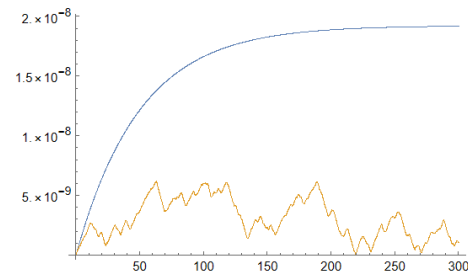
Tjit= 0.06



{1.50045 × 10⁸, 1.38855 × 10⁻¹²}
 {1.50045 × 10⁸, 1.45411 × 10⁻¹³}

{1., 0.104722}

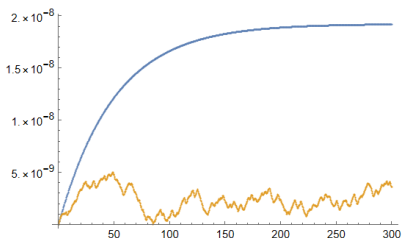
Tjit= 0.12



{7.5045 × 10⁷, 6.94365 × 10⁻¹³}
 {7.5045 × 10⁷, 3.01755 × 10⁻¹⁴}

{1., 0.0434577}

Tjit= 0.24

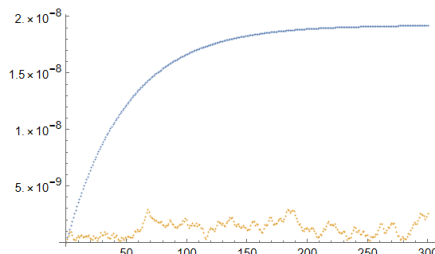


{3.7545 × 10⁷, 3.47274 × 10⁻¹³}
 {3.7545 × 10⁷, 8.39291 × 10⁻¹⁵}

{1., 0.024168}

Power
Suppression

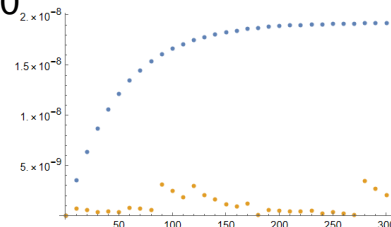
Tjit= 1



{9045050, 8.34857 × 10⁻¹⁴}
 {9045050, 5.7443 × 10⁻¹⁶}

{1., 0.00688058}

Tjit= 10



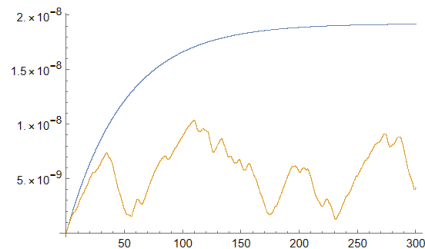
{945500, 8.51417 × 10⁻¹⁵}
 {945500, 6.53744 × 10⁻¹⁷}

{1., 0.00767831}



Tjit-Dependence (5 min runs); Rand[NormDist[0,3]]

Tjit= 0.03



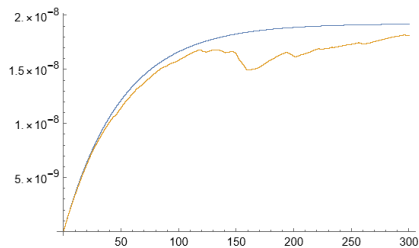
$[3.00045 \times 10^8, 2.77691 \times 10^{-12}]$

$[3.00045 \times 10^8, 3.65571 \times 10^{-13}]$

$[1., 0.131647]$

Power
Suppression

Tjit= 0.003



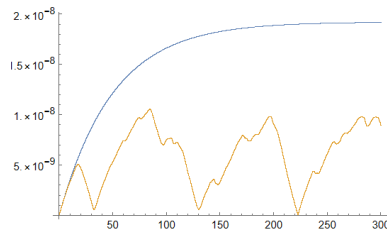
$[3.00005 \times 10^9, 2.77674 \times 10^{-11}]$

$[3.00005 \times 10^9, 2.29419 \times 10^{-11}]$

$[1., 0.826217]$

Power
Suppression

Tjit= 0.015

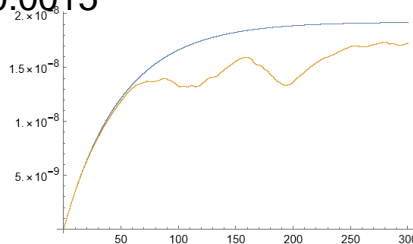


$[6.00045 \times 10^8, 5.55363 \times 10^{-12}]$

$[6.00045 \times 10^8, 8.60076 \times 10^{-13}]$

$[1., 0.154867]$

Tjit= 0.0015



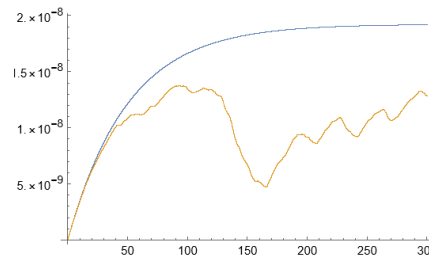
$[6.00005 \times 10^9, 5.55346 \times 10^{-11}]$

$[6.00005 \times 10^9, 3.96694 \times 10^{-11}]$

$[1., 0.714318]$

$[1., 0.714318]$

Tjit= 0.0075

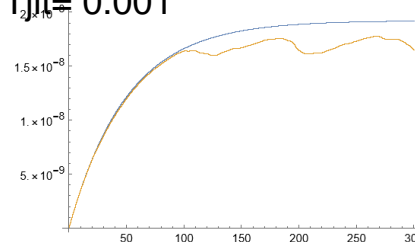


$[1.20005 \times 10^9, 1.11071 \times 10^{-11}]$

$[1.20005 \times 10^9, 4.22738 \times 10^{-12}]$

$[1., 0.380602]$

Tjit= 0.001



$[9.00005 \times 10^9, 8.33019 \times 10^{-11}]$

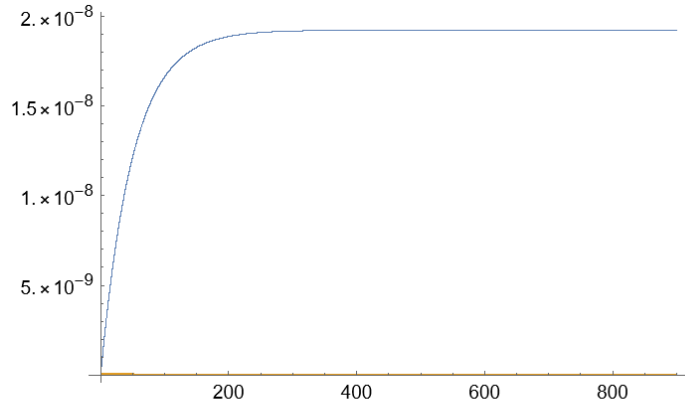
$[9.00005 \times 10^9, 7.08939 \times 10^{-11}]$

$[1., 0.851049]$

$[1., 0.851049]$



Fixed Offset– Power Suppression



$\{8.10041 \times 10^9, 1.01703 \times 10^{-11}\}$

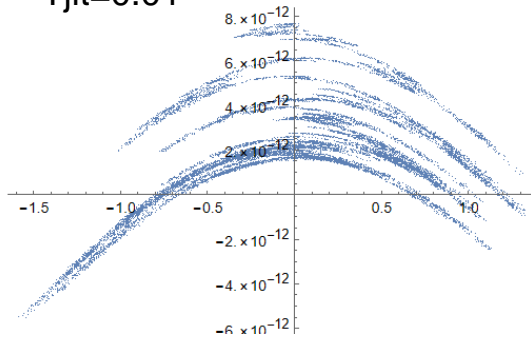
$\{8.10041 \times 10^9, 7.49701 \times 10^{-17}\}$

$\{1., 7.37147 \times 10^{-6}\}$

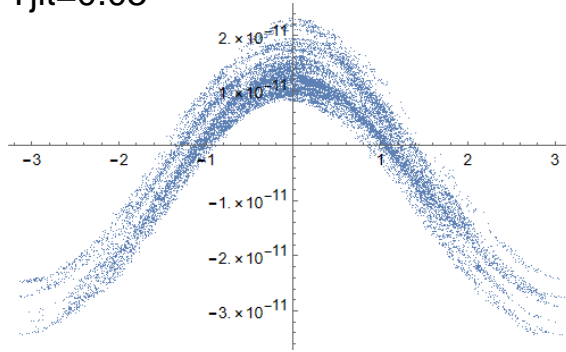


Phase vs Power, Tjit Dependence

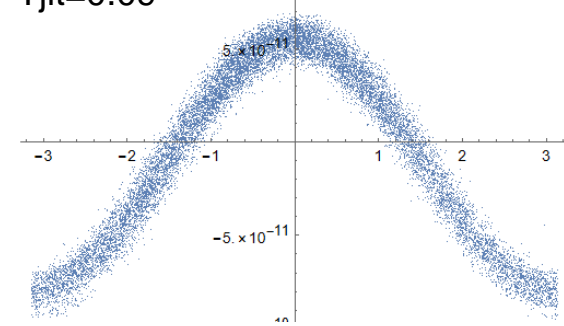
Tjit=0.01



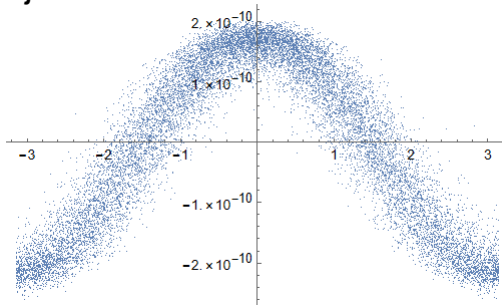
Tjit=0.03



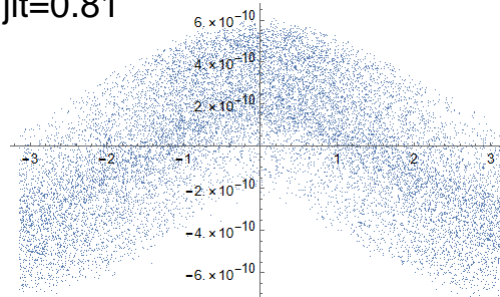
Tjit=0.09



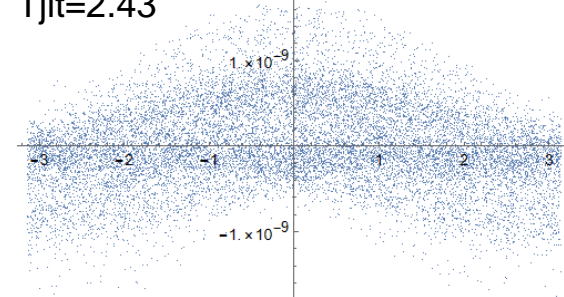
Tjit=0.27



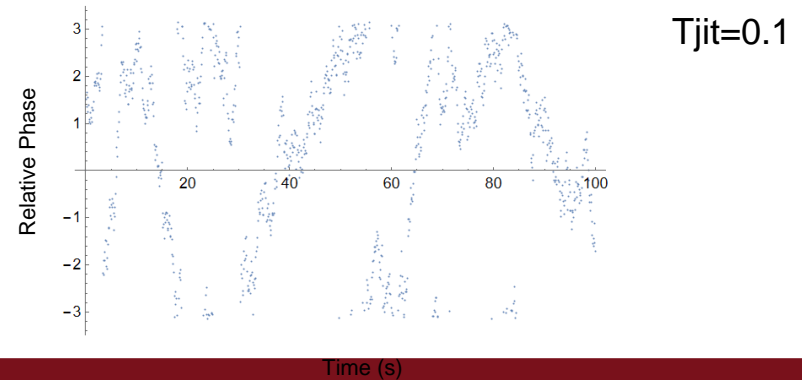
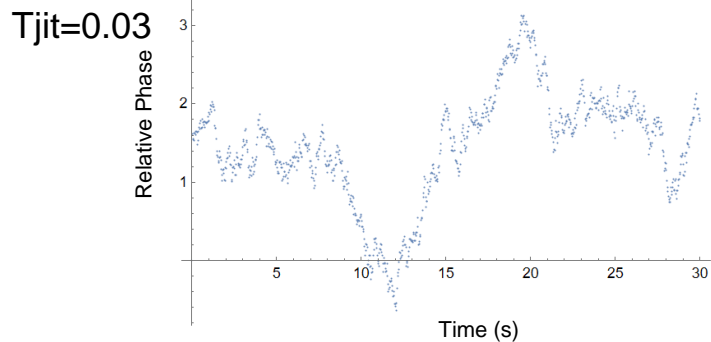
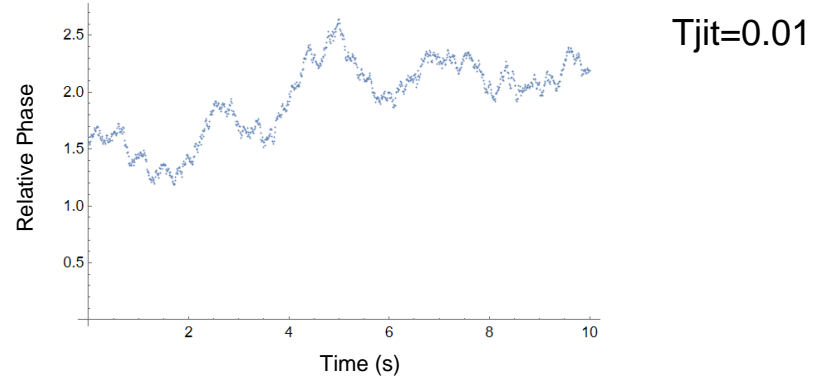
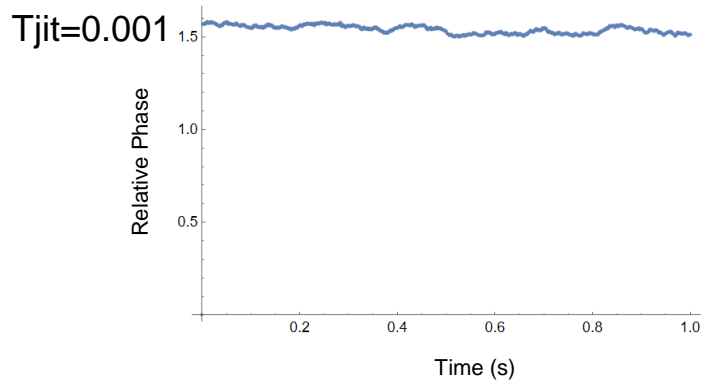
Tjit=0.81



Tjit=2.43

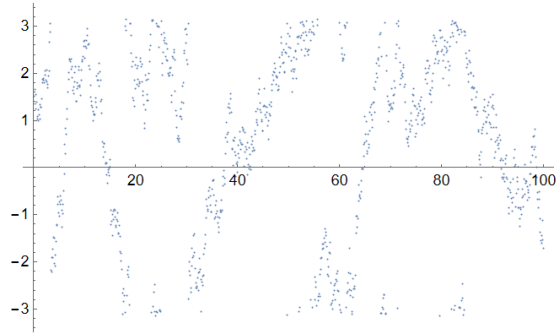


Tjit Dependence of Relative Phase

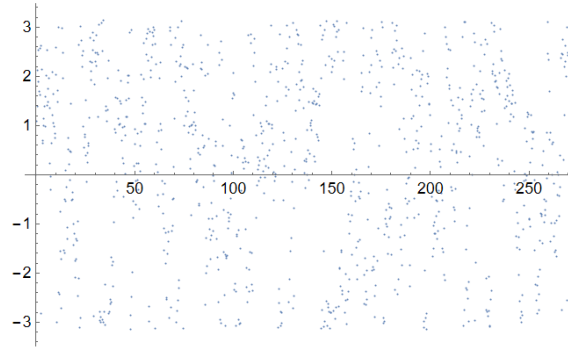


Tjit Dependence of Relative Phase

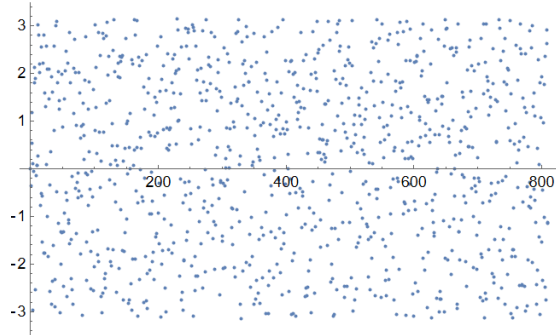
Tjit=0.1



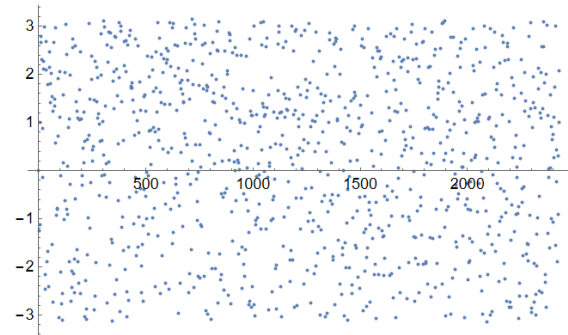
Tjit=0.27



Tjit=0.81



Tjit=2.43





UNIVERSITY OF MINNESOTA

Driven to Discover[®]

Crookston Duluth Morris Rochester Twin Cities

The University of Minnesota is an equal opportunity educator and employer.